University of Zurich[UZH]

Zurich Open Repository and Archive
University of Zurich
University Library
Strickhofstrasse 39
CH-8057 Zurich
www.zora.uzh.ch

Year: 2019

Priming anti-tumor immunity by radiotherapy: Dying tumor cell-derived DAMPs trigger endothelial cell activation and recruitment of myeloid cells

Krombach, Julia ; Hennel, Roman ; Brix, Nikko ; Orth, Michael ; Schoetz, Ulrike ; Ernst, Anne ; Schuster, Jessica ; Zuchtriegel, Gabriele ; Reichel, Christoph A ; Bierschenk, Susanne ; Sperandio, Markus ; Vogl, Thomas ; Unkel, Steffen ; Belka, Claus ; Lauber, Kirsten

Abstract: The major goal of radiotherapy is the induction of tumor cell death. Additionally, radiotherapy can function as cancer vaccination by exposing tumor antigens and providing adjuvants for anti-tumor immune priming. In this regard, the mode of tumor cell death and the repertoire of released damage-associated molecular patterns (DAMPs) are crucial. However, optimal dosing and fractionation of radiotherapy remain controversial. Here, we examined the initial steps of anti-tumor immune priming by different radiation regimens (20 Gy, 4 × 2 Gy, 2 Gy, 0 Gy) with cell lines of triple-negative breast cancer and . Previously, we have shown that especially high single doses (20 Gy) induce a delayed type of primary necrosis with characteristics of mitotic catastrophe and plasma membrane disintegration. Now, we provide evidence that protein DAMPs released by these dying cells stimulate sequential recruitment of neutrophils and monocytes . Key players in this regard appear to be endothelial cells revealing a distinct state of activation upon exposure to supernatants of irradiated tumor cells as characterized by high surface expression of adhesion molecules and production of a discrete cytokine/chemokine pattern. Furthermore, irradiated tumor cell-derived protein DAMPs enforced differentiation and maturation of dendritic cells as hallmarked by upregulation of co-stimulatory molecules and improved T cell-priming. Consistently, a recurring pattern was observed: The strongest effects were detected with 20 Gy-irradiated cells. Obviously, the initial steps of radiotherapy-induced anti-tumor immune priming are preferentially triggered by high single doses - at least in models of triple-negative breast cancer.

DOI: https://doi.org/10.1080/2162402X.2018.1523097

Posted at the Zurich Open Repository and Archive, University of Zurich
ZORA URL: https://doi.org/10.5167/uzh-165307
Journal Article
Published Version

The following work is licensed under a Creative Commons: Attribution 4.0 International (CC BY 4.0) License.

Originally published at:
Krombach, Julia; Hennel, Roman; Brix, Nikko; Orth, Michael; Schoetz, Ulrike; Ernst, Anne; Schuster, Jessica; Zuchtriegel, Gabriele; Reichel, Christoph A; Bierschenk, Susanne; Sperandio, Markus; Vogl,

Thomas; Unkel, Steffen; Belka, Claus; Lauber, Kirsten (2019). Priming anti-tumor immunity by radiotherapy: Dying tumor cell-derived DAMPs trigger endothelial cell activation and recruitment of myeloid cells. OncoImmunology, 8:e1523097.
DOI: https://doi.org/10.1080/2162402X.2018.1523097

OncoImmunology

ISSN: (Print) 2162-402X (Online) Journal homepage: https://www.tandfonline.com/loi/koni20

Priming anti-tumor immunity by radiotherapy: Dying tumor cell-derived DAMPs trigger endothelial cell activation and recruitment of myeloid cells

Julia Krombach, Roman Hennel, Nikko Brix, Michael Orth, Ulrike Schoetz, Anne Ernst, Jessica Schuster, Gabriele Zuchtriegel, Christoph A. Reichel, Susanne Bierschenk, Markus Sperandio, Thomas Vogl, Steffen Unkel, Claus Belka & Kirsten Lauber

To cite this article: Julia Krombach, Roman Hennel, Nikko Brix, Michael Orth, Ulrike Schoetz, Anne Ernst, Jessica Schuster, Gabriele Zuchtriegel, Christoph A. Reichel, Susanne Bierschenk, Markus Sperandio, Thomas Vogl, Steffen Unkel, Claus Belka & Kirsten Lauber (2019) Priming anti-tumor immunity by radiotherapy: Dying tumor cell-derived DAMPs trigger endothelial cell activation and recruitment of myeloid cells, OncoImmunology, 8:1, e1523097, DOI: 10.1080/2162402X.2018.1523097

To link to this article: https://doi.org/10.1080/2162402X.2018.1523097

© 2019 The Author(s). Published with license by Taylor & Francis Group, LLC

View supplementary material

Published online: 02 Nov 2018.

Submit your article to this journal

Article views: 319

View Crossmark data

Full Terms & Conditions of access and use can be found at https://www.tandfonline.com/action/journalInformation?journalCode=koni20

ONCOIMMUNOLOGY
2019, VOL. 8, NO. 1, e1523097 (15 pages)
https://doi.org/10.1080/2162402X.2018.1523097

Taylor & Francis
Taylor & Francis Group

ORIGINAL RESEARCH

OPEN ACCESS Check for updates

Priming anti-tumor immunity by radiotherapy: Dying tumor cell-derived DAMPs trigger endothelial cell activation and recruitment of myeloid cells

Julia Krombach[a*], Roman Hennel[a*], Nikko Brix[a], Michael Orth[a,b,c], Ulrike Schoetz[a,d], Anne Ernst[a,e], Jessica Schuster[a], Gabriele Zuchtriegel[f,g,h], Christoph A. Reichel[f,g], Susanne Bierschenk[g], Markus Sperandio[g], Thomas Vogl[i], Steffen Unkel[j], Claus Belka[a,b,k], and Kirsten Lauber[a,b,k]

[a]Department of Radiation Oncology, University Hospital, Munich, Germany; [b]German Cancer Consortium (DKTK), Munich, Germany; [c]German Cancer Research Center (DKFZ), Heidelberg, Germany; [d]Department of Radiotherapy and Radiooncology, Philipps-University Marburg, University Hospital Gießen and Marburg, Marburg, Germany; [e]Division of Radiation and Cancer Biology, Department of Radiation Oncology, Stanford University School of Medicine, Stanford, California, USA; [f]Department of Otorhinolaryngology, University Hospital, Munich, Germany; [g]Walter Brendel Centre of Experimental Medicine, University Hospital, Munich, Germany; [h]Translational research in haematology/oncology, Institute of Experimental Infectious Diseases and Cancer Research, Division of the University Children's Hospital of Zurich, Zurich, Switzerland; [i]Institute of Immunology, University of Münster, Münster, Germany; [j]Department of Medical Statistics, University Medical Center, Goettingen, Germany; [k]Clinical Cooperation Group 'Personalized Radiotherapy in Head and Neck Cancer' Helmholtz Center Munich, German Research Center for Environmental Health GmbH, Neuherberg, Germany

ABSTRACT

The major goal of radiotherapy is the induction of tumor cell death. Additionally, radiotherapy can function as *in situ* cancer vaccination by exposing tumor antigens and providing adjuvants for anti-tumor immune priming. In this regard, the mode of tumor cell death and the repertoire of released damage-associated molecular patterns (DAMPs) are crucial. However, optimal dosing and fractionation of radiotherapy remain controversial. Here, we examined the initial steps of anti-tumor immune priming by different radiation regimens (20 Gy, 4 × 2 Gy, 2 Gy, 0 Gy) with cell lines of triple-negative breast cancer *in vitro* and *in vivo*. Previously, we have shown that especially high single doses (20 Gy) induce a delayed type of primary necrosis with characteristics of mitotic catastrophe and plasma membrane disintegration. Now, we provide evidence that protein DAMPs released by these dying cells stimulate sequential recruitment of neutrophils and monocytes *in vivo*. Key players in this regard appear to be endothelial cells revealing a distinct state of activation upon exposure to supernatants of irradiated tumor cells as characterized by high surface expression of adhesion molecules and production of a discrete cytokine/chemokine pattern. Furthermore, irradiated tumor cell-derived protein DAMPs enforced differentiation and maturation of dendritic cells as hallmarked by upregulation of co-stimulatory molecules and improved T cell-priming. Consistently, a recurring pattern was observed: The strongest effects were detected with 20 Gy-irradiated cells. Obviously, the initial steps of radiotherapy-induced anti-tumor immune priming are preferentially triggered by high single doses – at least in models of triple-negative breast cancer.

ARTICLE HISTORY
Received 21 May 2018
Revised 4 September 2018
Accepted 8 September 2018

KEYWORDS
Radiotherapy; anti-tumor immunity; abscopal effects of radiotherapy; DAMPs; endothelial cell activation; APC recruitment; cancer immunotherapy

Introduction

The induction of tumor cell death and the abrogation of clonogenic survival are considered the major determinants in radio- and/or chemotherapy of cancer.[1] However, meanwhile it is well accepted that immune mechanisms contribute to the therapeutic outcome and that the mode of tumor cell death determines if and to which extent irradiation converts the tumor into an *in situ* vaccine.[2–4] Apart from tumor antigens which need to be made accessible to the immune system, the presence of adjuvants orchestrating the recruitment, differentiation, and activation of antigen-presenting cells (APCs) in the tumor microenvironment is of pivotal importance for the successful priming of anti-tumor immunity.[5,6] In this regard, tumor cells undergoing immunogenic forms of cell death are known to release damage-associated molecular patterns (DAMPs), including heat shock protein 70 (HSP70), high mobility group box1 (HMGB1), and ATP, thereby supporting the recruitment and maturation of APCs.[7–10] However, the mode of cell death induced by ionizing irradiation is not uniform, and it clearly depends on the irradiation dose, the fractionation regimen, and the genetic repertoire of the irradiated cells.[3,10] Proliferating cells of the hematopoietic system predominantly undergo apoptosis upon irradiation, as characterized by externalization of phosphatidylserine, membrane blebbing, chromatin condensation, and DNA fragmentation, while the integrity of the plasma membrane remains intact.[11] If apoptotic cells are not removed in time by

CONTACT Kirsten Lauber kirsten.lauber@med.uni-muenchen.de Department of Radiation Oncology, University Hospital, Ludwig-Maximilians-Universität München, Marchioninistrasse 15, 81377 Munich, Germany

*Both authors share equal first authorship

Color versions of one or more of the figures in the article can be found online at www.tandfonline.com/koni.

The supplementary data for this article can be accessed here.

© 2019 The Author(s). Published with license by Taylor & Francis Group, LLC
This is an Open Access article distributed under the terms of the Creative Commons Attribution-NonCommercial-NoDerivatives License (http://creativecommons.org/licenses/by-nc-nd/4.0/), which permits non-commercial re-use, distribution, and reproduction in any medium, provided the original work is properly cited, and is not altered, transformed, or built upon in any way.

professional or non-professional phagocytes, they progress into secondary, post-apoptotic necrosis: The integrity of the plasma membrane collapses, and intracellular contents, including DAMPs, are released.[3,12] In cells of epithelial origin, the extent of apoptosis induction upon irradiation is rather limited. As long as cell cycle checkpoint function is maintained, epithelial cells exit the cell cycle into cellular senescence as hallmarked by upregulation of cyclin-dependent kinase inhibitors, such as p16, p21, and p27, and expression of senescence-associated β-galactosidase.[13] If cell cycle checkpoint function is impaired, persisting DNA damage will be transferred into the next round of mitosis leading to aberrant chromosomal segregation. Upon 2–3 rounds of anomalous mitosis, highly aneuploid cells with huge and/or multiple nuclei and abnormal morphology emerge. They may subsequently undergo a delayed form of apoptosis. More frequently however, programmed necroptosis or uncontrolled necrosis are observed, encompassing plasma membrane permeabilization and/or rupture, cellular disintegration, and leakage of the intracellular contents into the surroundings.[10,14] In parallel to the different modes of cell death, the induction of systemic immune responses by local radiotherapy – known as radiotherapy's abscopal effects – varies widely with the model systems and the radiation regimen employed.[6,15–17] Investigations in different mouse tumor models revealed that radiotherapy-induced anti-tumor immune reactions, which are essentially dependent on type-I interferons (produced by the cyclic GMP-AMP synthase (cGAS)/stimulator of interferon genes (STING) axis), APCs, and cytotoxic $CD8^+$ T cells, are exclusively stimulated by high single doses (10–20 Gy).[18–23] On the contrary, a recent study suggests that 3 × 8 Gy may be optimal.[24] Clinically, abscopal tumor lesion regression remains rare, most likely because comparable super-hypofractionated protocols (fractions of >5 Gy) are rarely used in the radiotherapeutic routine.

Systematic analyses addressing the immunological consequences of different radiation regimens are scarce. Therefore, the present study was designed to examine the initial steps of anti-tumor immune priming by radiotherapy with specific focus on endothelial cell activation, recruitment and activation of APCs in the context of different radiation regimens. We chose cell lines of triple-negative breast cancer (histologically negative for estrogen, progesterone, and Her2/neu receptors) as our model systems, since this breast cancer subtype is associated with particularly poor prognosis. No targeted therapy is currently available, and due to early and extensive metastasis formation, patients with this subtype may have relevant benefits from radiotherapy-induced anti-tumor immune responses.[25] Interestingly, a recent study provided evidence that the expression levels of pro-necrotic signaling genes correlate with the ones of intra-tumoral immune cell subsets suggesting that necrotic processes may be involved in controlling intra-tumoral immune responses in human breast cancer.[26]

Previously, we have shown that particularly high single dose irradiation at 20 Gy stimulates a late-onset type of primary necrosis in triple-negative breast cancer cells revealing a chaotic morphology with features of mitotic catastrophe and plasma membrane disintegration.[11,27] Here, culture supernatants of these dying cells were analyzed for their effects on endothelial cell activation as well as the recruitment and activation of APCs *in vitro* and *in vivo*. The results were compared to supernatants of 4 × 2 Gy-, 2 Gy-, and sham-irradiated cells. Our data show that high single dose irradiation leads to the release of protein DAMPs which trigger a distinct state of activation in endothelial cells as characterized by upregulation of adhesion molecules, and a cytokine/chemokine expression pattern dominated by IL-6, CXCL1, −2, −3, and CCL7, leading to sequential recruitment of neutrophils and monocytic cells *in vivo*. *In vitro*, the presence of these tumor cell-derived DAMPs enforced differentiation and maturation of human monocyte-derived dendritic cells (DCs), resulting in improved T cell activation.

Results

Irradiated tumor cell-derived DAMPs stimulate recruitment of neutrophils and monocytic cells in vivo

Previously, we have shown that γ-irradiation induces different forms of cell death in breast cancer cells depending on the radiation regimen and the genetic composition of the irradiated cells.[27] In triple-negative breast cancer cells, such as HCC1937 cells, we observed a delayed type of primary necrosis with chaotic morphology which was particularly prominent 4 days after irradiation with a high single dose of 20 Gy (Supplemental Figure 1,[27]).

In the present study, we examined the recruitment of myeloid cells by culture supernatants of irradiated tumor cells *in vivo*. We utilized an air pouch model, where supernatants of HCC1937 cells (harvested 4 days after irradiation at 0 Gy, 2 Gy, daily 2 Gy, and 20 Gy) were injected, and the dynamics of myeloid cell subset recruitment were analyzed in the air pouch lumen as well as in the air pouch skin (Figure 1(a)). Unconditioned culture medium served as negative control, and tumor necrosis factor (TNF) was used as positive control (Figure 1(b)). Hematoxylin/eosin (H&E) staining reproducibly demonstrated a well-defined structure of the air pouch skin (Figure 1(c)): Distant from the lumen, muscle and fat cells with small inner vessels were overlain by loose connective tissue covered by several cell layers with squamous epithelial morphology proximal to the pouch lumen. Polymorphonuclear neutrophils (PMNs) were observed to different extents inside the muscle, the connective tissue, and the squamous epithelial layer indicating active infiltration of PMNs from the small vessels into the pouch cavity. This was most obvious in pouches that had been treated with TNF, 4 × 2 Gy, and 20 Gy culture supernatants.

In order to dissect myeloid subsets and the time course of their infiltration, skin samples were subjected to confocal immunofluorescence microscopy (Figure 1(d)). $Ly6G^+$ neutrophils swiftly accumulated up to 6 h after injection. After 12 h, these neutrophils had gradually disappeared, and $F4/80^+$ monocytic/macrophagocytic cells were observed. The numbers of $F4/80^+$ cells further increased up to 24 h after supernatant injection.

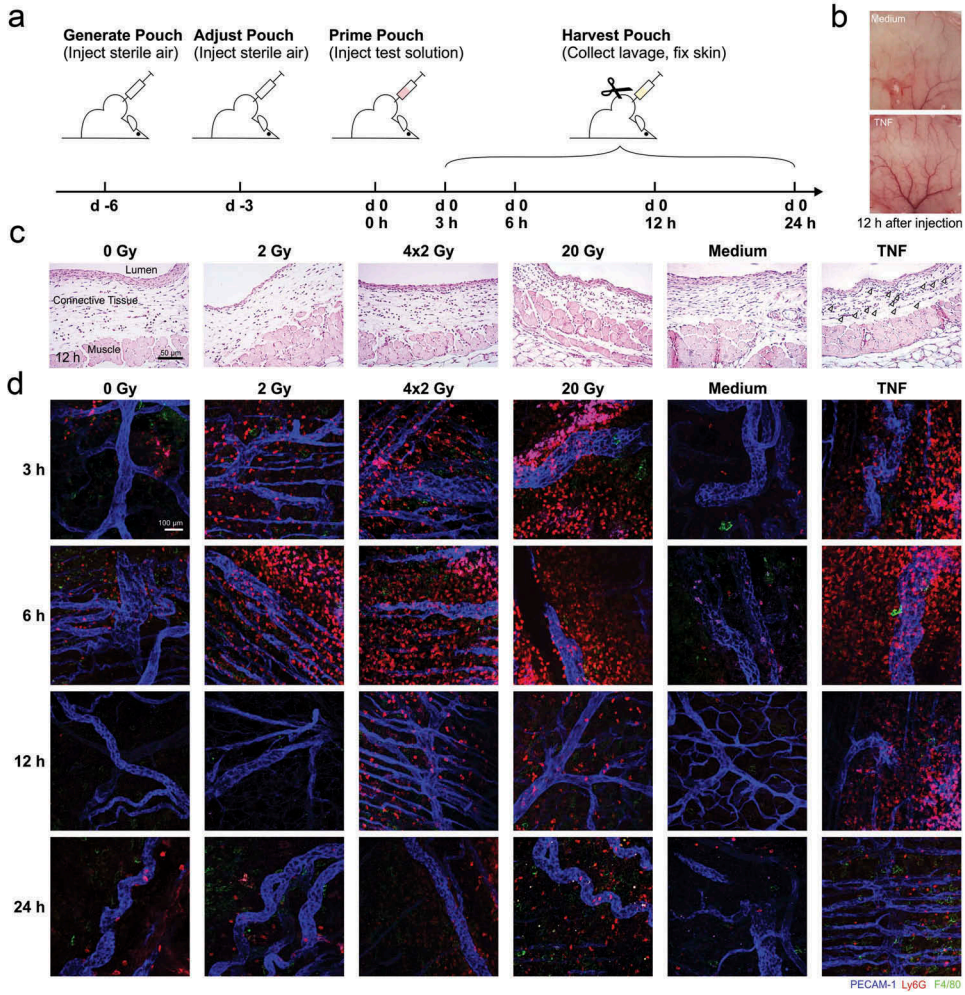

Figure 1. *In vivo* recruitment of myeloid cell subsets stimulated by supernatants of irradiated tumor cells in an air pouch model. (a) Schematic representation of the treatment sequence in air pouch experiments. (b) Representative photographs of native air pouch skin samples (luminal side) 12 h after injection of control medium or medium supplemented with 50 ng/ml TNF. (c) Paraffin sections (3 µm) of representative air pouch skin samples 12 h after injection of the indicated supernatants of irradiated HCC1937 cells or respective control stimuli (medium or 50 ng/ml TNF) were subjected to H&E-staining. 20x magnification, scale bar 50 µm. Arrowheads indicate PMNs in the TNF sample. (d) Exemplary air pouch skin samples were prepared, stained, and examined by confocal immunofluorescence microscopy. For the visualization of endothelial cells, neutrophils, and macrophages, immunostaining against PECAM-1 (blue), Ly6G (red), and F4/80 (green) was performed. 20x magnification, scale bar 100 µm.

Importantly, there were clear differences between the radiation regimens. The strongest effects were seen with supernatants of 20 Gy-irradiated cells.

Via flow cytometric analyses of the air pouch lavages we further characterized the recruited myeloid cells and quantified the dynamics of the infiltration process (Figure 2(a)). The number of recruited $CD45^+$ cells increased over time with a maximum 6 h after injection, followed by a decrease down to baseline levels. This was dominated by $Ly6G^+$ neutrophils and was strongest when supernatants of 20 Gy-irradiated cells were injected. Supernatants of 4 × 2 Gy- and 2 Gy-irradiated cells recruited lower levels of $CD45^+$ cells, while $CD45^+$ cells barely exceeded control levels when supernatants of non-irradiated cells were deployed. Apart from neutrophils, $Ly6C^{hi}$ and $Ly6C^{lo}$ monocytes were observed, yet in lower numbers. The infiltration kinetics of $Ly6C^{hi}$ and $Ly6C^{lo}$ monocytes were delayed as compared to those of $Ly6G^+$ neutrophils, and the maximal monocyte numbers were detected 12 h after supernatant injection. Again, highest cell numbers were found with supernatants of 20 Gy-irradiated cells. Virtually the same observations were made when supernatants of irradiated HCC1806 cells were employed in the air pouch model. Yet, here the difference between irradiation at 20 Gy and all other irradiation regimens was even more pronounced (Supplemental Figure 3).

Quantitative realtime PCR (qRT-PCR)-analyses of the air pouch skin samples confirmed the recruitment of myeloid cells stimulated by dying tumor cell-derived supernatants (Figure 2(b)). The kinetics of L-selectin mRNA levels, a leukocyte marker, paralleled the infiltration pattern as detected by flow cytometry and confocal microscopy. This was preceded by an early increase in mRNA expression of IL-6 and IL-1β and chemokines including CXCL1, −2, and −3. Obviously, cells in the air pouch skin

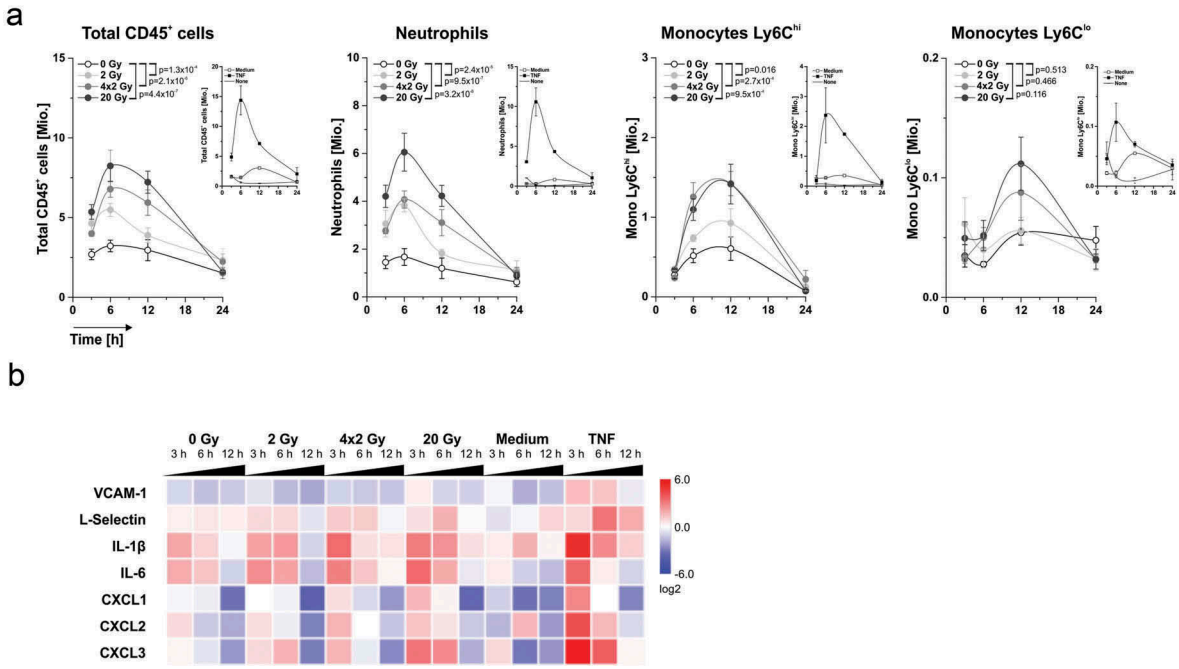

Figure 2. Dynamics of leukocyte recruitment and mRNA expression of crucial regulator molecules in the air pouch microenvironment. (a) Dynamics of leukocyte recruitment into the air pouch lumen. Air pouch lavages were collected at the indicated time points, and leukocyte subsets were analyzed by flow cytometry. Total cell numbers per pouch are shown (n = 6 animals for supernatants, n = 2 animals for the control stimuli medium or 50 ng/ml TNF). Means ± SEM are depicted, and *p*-values were calculated by two-way ANOVA with Bonferroni-Holm correction. (b) mRNA expression of key regulator molecules in the air pouch microenvironment. Air pouch skin samples (n = 6 animals for cell culture supernatants, n = 2 animals for the control stimuli medium or 50 ng/ml TNF) were subjected to realtime qRT-PCR. Results were normalized on a reference gene matrix of 18S rRNA, δ-ALAS, β-actin, α-tubulin, and PECAM-1, and calibrated on the medium-injected controls. Means of log2 expression values are depicted.

were stimulated to produce these mediators upon exposure to dying tumor cell-derived supernatants and thus are likely to orchestrate the directional recruitment of myeloid cells *in vivo*.

Endothelial cells are activated by protein DAMPs from irradiated tumor cells via contribution of toll-like receptor 4

Recruitment of leukocytes to sites of tissue damage and/or infection is highly dependent on the activation of endothelial cells. Activated endothelial cells express adhesion molecules and release and/or deposit chemokines on their surface in order to attract leukocytes and facilitate their extravasation.[28] Based on our observations in the air pouch model, the influence of irradiated tumor cells on endothelial cell activation was examined. To this end, human umbilical vein endothelial cells (HUVECs) were treated with supernatants of irradiated tumor cells, and surface expression of the adhesion molecules ICAM-1, VCAM-1, and E-selectin was visualized by immunofluorescence on native, non-fixed cells (Figure 3(a)). Clear differences between the radiation regimens were observed: Whereas no expression of adhesion molecules was detected on HUVECs exposed to supernatants of sham-irradiated cells, supernatants of 2 Gy- and 4 × 2 Gy-irradiated cells induced a moderate increase, and exposure to supernatants of 20 Gy-irradiated cells resulted in a strong upregulation. These observations were confirmed with supernatants of other breast cancer cell lines showing similar patterns of cell death induction upon irradiation (Supplemental Figure 4,[27]). The extent of ICAM-1 and E-selectin surface upregulation was quantified by fluorometric analyses and did further strengthen our microscopy findings with the most prominent effects being observed upon exposure to supernatants of 20 Gy-irradiated cells (Figure 3(b) and Supplemental Figure 5(a)). Biochemical characterization revealed that the molecular entities responsible for stimulation of adhesion molecule upregulation are protein DAMPs as they were sensitive to proteinase K digestion and exhibited an apparent molecular weight of >10 kDa (Figure 3(c) and Supplemental Figure 5(b)). Potential candidates for these protein DAMPs are HSP70, HMGB1, and S100A8/A9 dimer, since all of them were time- and dose-dependently released by irradiated tumor cells as detected by ELISA measurements (Figure 3(d)). While the lowest concentrations were found in the non-irradiated controls, irradiation at 2 Gy and 4 × 2 Gy resulted in a clear increase in DAMP concentration. Importantly, highest concentrations were measured after irradiation at 20 Gy, thus matching the pattern of endothelial cell activation. Protein DAMP release was confirmed in supernatants of other irradiated triple-negative breast cancer cell lines (Supplemental Figure 6).

Next, we focused on the corresponding receptors which mediate HUVEC activation. As such, toll-like receptor 4 (TLR4) and/or the TLR2/TLR4 heterodimer represent common receptors for HMGB1, HSP70, and S100A8/A9.[29–31] Importantly, when TLR4 was blocked using the antagonist RS-LPS, HUVEC activation as measured by upregulation of ICAM-1 surface expression was strongly, yet not completely inhibited (Supplemental Figure 7A). Reporter cell lines confirmed the activation of TLR4 and TLR2 by supernatants of

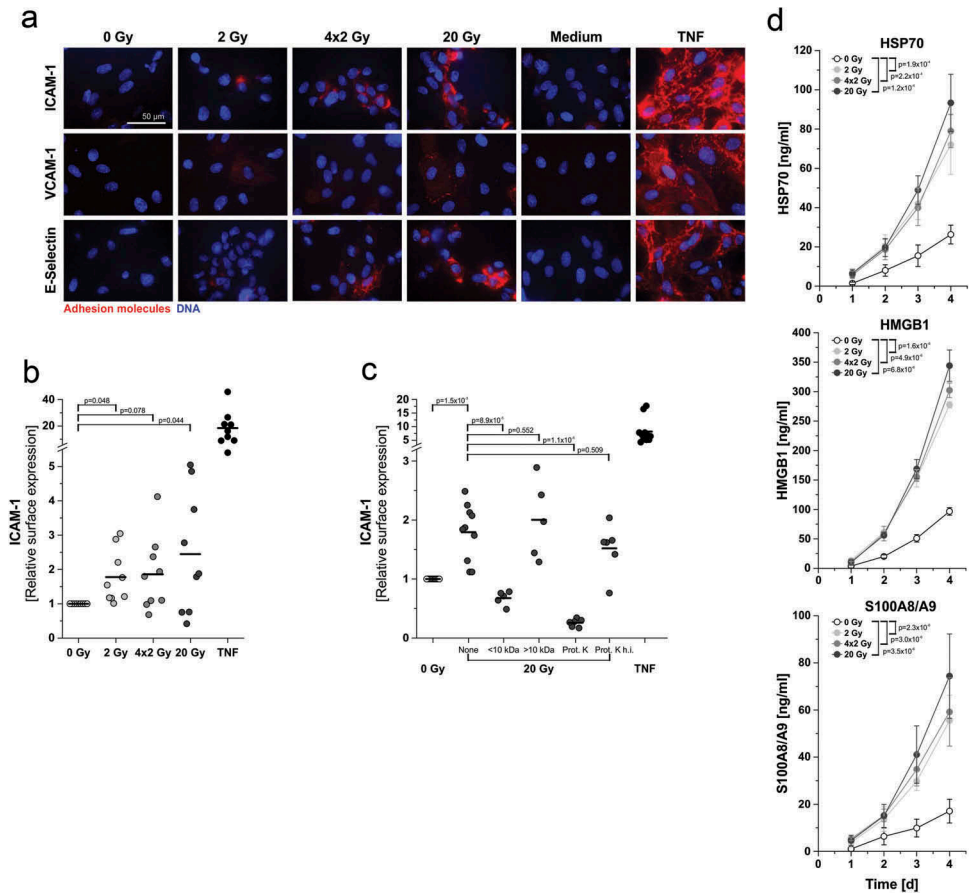

Figure 3. *In vitro* endothelial cell activation and upregulation of adhesion molecule surface expression are mediated by protein DAMPs derived from irradiated tumor cells. (a) Representative photographs of immunofluorescent adhesion molecule surface staining on HUVECs 4 h after exposure to supernatants of irradiated HCC1937 cells. Surface expression was visualized by immunofluorescence microscopy on native, non-fixed HUVECs. Medium and TNF (50 ng/ml) served as controls. 63x magnification, scale bar 50 µm. (b) Quantitation of ICAM-1 surface expression on HUVECs by fluorometric measurement. HUVECs were treated as in (a) and subjected to native immunofluorescence staining. Staining intensities were quantified by fluorometric measurement, and x-fold expression levels were calculated as the means of fluorescence intensities subtracted by the corresponding isotype controls and normalized to the 0 Gy samples (n = 9 independent experiments). *p*-values were calculated by unpaired Student's *t*-tests with Bonferroni-Holm correction. (c) Biochemical characterization of the molecular entities mediating upregulation of ICAM-1 expression. Supernatants of 20 Gy-irradiated HCC1937 cells were applied to membrane centrifugation (molecular weight cut-off 10 kDa) or proteinase K treatment prior to incubation with HUVECs. ICAM-1 surface expression was measured as in (b) (n = 5–10 independent experiments). Group comparison was performed by unpaired Student's *t*-test with Bonferroni-Holm correction. (d) HSP70, HMGB1, and S100A8/A9 were quantified in supernatants of irradiated HCC1937 cells by ELISA. Concentrations were calculated on the basis of standard curves. Means ± SD of 3 (HSP70), 4 (HMGB1), or 5 (S100A8/A9) independent experiments are shown. Group comparison was carried out by two-way ANOVA with Bonferroni-Holm correction.

irradiated breast cancer cells (Supplemental Figure 7B, C). Hence, TLR4 and/or the TLR2/4 heterodimer are activated by protein DAMPs released from irradiated breast cancer cells and appear to be involved in the regulation of endothelial cell activation. Nevertheless, further receptors, including RAGE and members of the scavenger receptor family, which also have been reported as receptors for dying cell-derived protein DAMPs, may additionally contribute.[32]

Upregulation of adhesion molecule expression in HUVECs was also detected on the mRNA level as confirmed by qRT-PCR analyses (Figure 4(a)). This was accompanied by upregulation of diverse chemokines and cytokines involved in the recruitment process whose expression thus constitutes another hallmark of endothelial cell activation. Intriguingly, although there were several similarities, the activation pattern of endothelial cells exposed to supernatants of irradiated cells was clearly distinct from the one stimulated by TNF. Dimensionality reduction by principal component analysis revealed three activation states, (i) the TNF-positive control samples, (ii) the 20 Gy-irradiated samples, and (iii) the remaining samples, including the other radiation regimens and the medium control (Figure 4(b)). The biplot diagram clearly shows that IL-6, CXCL1, −2, and to a lesser extent also CXCL3 and CCL7 represent the variables with the highest loadings for PC2 which predominantly separates the 20 Gy samples from all others. Accordingly, they appear to be the major determinants of the HUVEC response towards supernatants of irradiated tumor cells. Multiplex-ELISA measurements confirmed the increased production of these cytokines and chemokines on the secretome level (Figure 4(c)). Elevated concentrations of IL-6, CXCL1, CXCL2, and CCL7 were secreted by HUVECs after incubation with conditioned media of irradiated tumor cells in comparison to sham-irradiated controls or unconditioned medium, respectively. The same trend was observed for CXCL8, CCL2, and IL-1β.

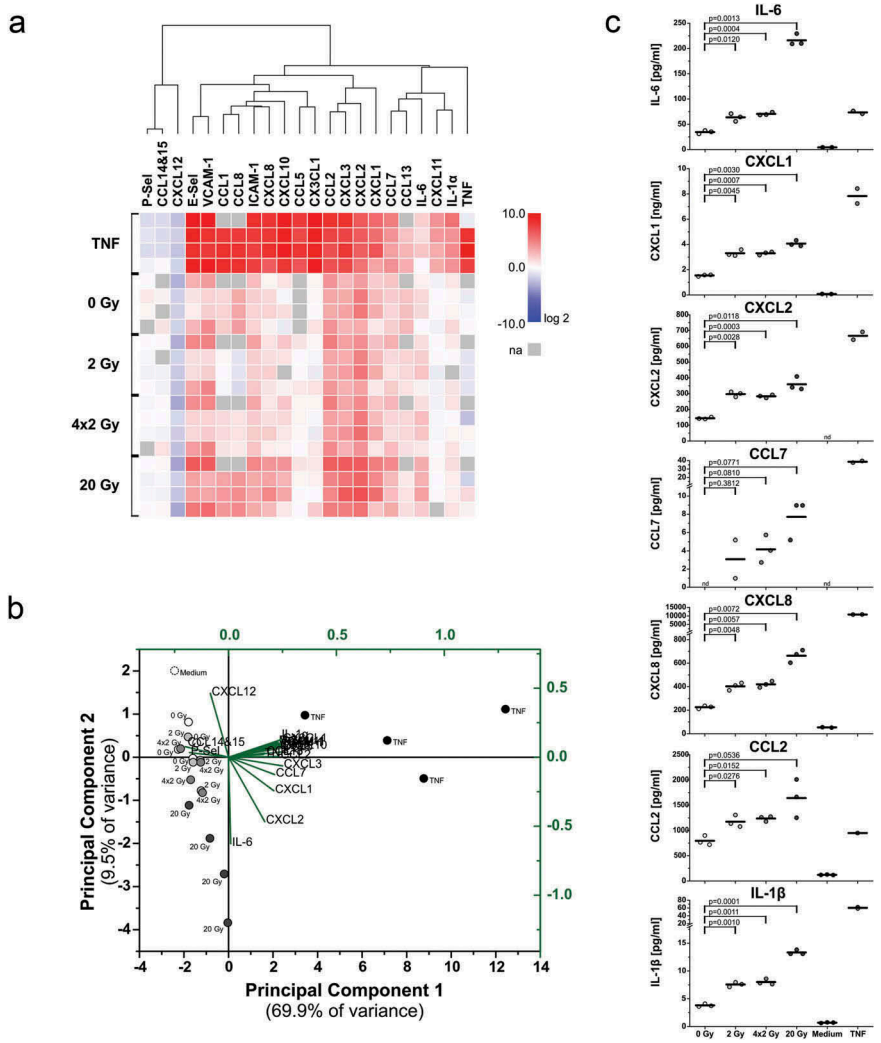

Figure 4. Upregulation of cytokines and chemokines in endothelial cells upon exposure to supernatants of irradiated tumor cells. (a) mRNA expression levels of crucial adhesion molecules, cytokines, and chemokines. HUVECs were incubated with supernatants of irradiated HCC1937 cells for 4 h as in Figure 3. mRNA expression levels were determined by qRT-PCR, normalized on a reference gene matrix of 18S rRNA, β_2-microglobulin, and δ-ALAS, and calibrated on the respective medium-treated samples. TNF (50 ng/ml) served as positive control. Unsupervised hierarchical clustering of log2 expression values of 4 independent experiments is depicted (na indicates not assessed). (b) Principal component analysis (PCA) of mRNA expression data from (a). The biplot shows the scores of the samples (black coordinate system) and the scaled loadings of the input variables (green coordinate system) in the subspace of the first two principal components. (c) Cytokines and chemokines released from HUVECs were measured by multiplex-ELISAs after exposure to supernatants of irradiated HCC1937 cells for 4 h and incubation in fresh medium for two more hours. Concentrations were calculated on the basis of standard curves. n = 3 independent experiments are shown (nd indicates not detectable), and *p*-values were determined by unpaired Student's *t*-tests with Bonferroni-Holm correction.

Protein levels of secreted cytokines and chemokines showed analogous patterns as the mRNA levels. The strongest increase was detected in response to supernatants of 20 Gy-irradiated cells, and weaker effects were seen with supernatants of 4 × 2 Gy- and 2 Gy-irradiated cells.

Functionally, HUVEC activation was paralleled by improved adhering and crawling of PMNs in *in vitro* flow chamber experiments (Supplemental Figure 8). Yet, this did not reach statistical significance.

Protein DAMPs from irradiated tumor cells enforce differentiation and maturation of APCs

In the air pouch experiments, we did not detect relevant recruitment of APCs, such as DCs (Figure 2(a) and Supplemental Figure 3). Nevertheless, Ly6C^{hi} monocytic cells have the potential to differentiate into several subsets with antigen-presenting and cross-presenting capacity.[33] This requires upregulation of peptide-presenting MHC class II and class I molecules as well as enhanced expression of co-stimulatory signals, including CD80, CD86, and CD40, which are necessary for proper T cell activation via CD28 and CD40L.[34] Along these lines, it becomes increasingly evident that monocytic cells can give rise to a population of monocytic APCs which are of importance for the stimulation of anti-tumor immune mechanisms during cancer therapy – at least in mouse tumor models.[8,35,36] For anthracycline-based chemotherapy, it has already been shown that dying cancer cells can stimulate the differentiation of recruited monocytes into antigen-presenting DCs.[8] Thus, we hypothesized that similar effects on DC differentiation and maturation may be induced by irradiated, dying cancer cells.

In the differentiation approach, primary human monocytes were stimulated with supernatants of irradiated tumor cells

followed by *in vitro* differentiation into DCs with IL-4 and GM-CSF for 5 days. Characteristic DC markers of the immunological synapse were monitored by flow cytometry. The co-stimulatory ligands CD80 and CD86, the DC maturation marker CD83, the co-activating receptor CD40, and the MHC class II molecule HLA-DR were increased after monocyte exposure to supernatants of irradiated tumor cells (Figure 5(a)). The most prominent effects were observed in case of CD80 surface expression. Supernatants of 20 Gy-irradiated cells stimulated the strongest increase, while this was reduced with supernatants of 4 × 2 Gy- and 2 Gy-irradiated cells. Biochemical characterization of the responsible DAMPs was performed analogously to the experiments on endothelial cell activation (Figure 3(c)). Proteins >10 kDa were again identified as the relevant mediators (Figure 5(b)).

Next, the influence of irradiated tumor cell-derived DAMPs on DC maturation was examined. To this end, DCs differentiated for 5 days from primary human monocytes were exposed to supernatants of irradiated tumor cells for 2 days. The changes in the expression pattern of DC markers were similar to the ones observed in the differentiation approach (Figure 5(c)). Again, the strongest upregulation was detected in case of CD80. Supernatants of 20 Gy-irradiated cells induced the highest increase in CD80 expression, and protein DAMPs >10 kDa were responsible for the upregulation (Figure 5(d)).

Effector functions of APCs are improved after exposure to irradiated tumor cells

Upon recruitment and differentiation of APCs, uptake of antigen material is the next step in generating an anti-tumor immune response.[5] We examined tumor antigen uptake by co-incubating DCs with tumor cells in increasing target:effector ratios. Phagocytosis was analyzed by flow cytometry and live cell imaging (Figure 6(a) and Supplemental Movies). As expected, the percentage of phagocytosing DCs increased with rising target:effector ratios, and irradiated prey cells were significantly better engulfed than non-irradiated controls. Addition of the actin polymerization inhibitor cytochalasin D prior to the phagocytosis assay confirmed active internalization (Figure 6(b)).

Finally, we investigated the activation of T cells by APCs upon exposure to irradiated tumor cell supernatants. Mixed leukocyte reactions of DCs with allogeneic T cells were set up, and proliferation of CFSE-labeled $CD4^+$ and $CD8^+$ T cells was measured by flow cytometry (Figure 6(c)). Whereas $CD4^+$ T cell proliferation was only slightly affected, proliferation of $CD8^+$ T cells was significantly increased when DCs had been differentiated in the presence of supernatants of 20 Gy-irradiated tumor cells.

Discussion

Radiotherapy is a cornerstone of cancer treatment and can significantly prolong overall survival – not only in breast cancer.[37] In addition to its direct tumoricidal effects, radiotherapy is known to induce distinct changes in the tumor microenvironment, particularly in the leukocyte compartment.[38] Meanwhile, it is well acknowledged that anti-tumor immune mechanisms can be stimulated by radiotherapy in the sense of an *in situ* cancer vaccination.[4,6] However, the optimal dosing and fractionation regimen for the induction of anti-tumor immunity by ionizing irradiation remain controversial.[21,39–41]

In the present study, we systematically analyzed the initial steps of anti-tumor immune priming by radiotherapy in complementary *in vivo* and *in vitro* models. We focused on triple-negative breast cancer cells and examined the effects of dying tumor cell-derived DAMPs on endothelial cell activation, as well as on the recruitment and differentiation of APCs in the context of different irradiation doses and fractionation regimens.

The activation of endothelial cells is a prerequisite for immune cell trafficking.[28] Endothelial cells upregulate adhesion molecules such as E-selectin, ICAM-1, and VCAM-1, and release and/or deposit chemokines on their cell surface in order to facilitate the extravasation of leukocytes from the bloodstream into the tissue.[28] We observed a strong upregulation of E-selectin, ICAM-1, and VCAM-1 on endothelial cells mediated by protein DAMPs derived from irradiated tumor cells that was part of a distinct activation pattern – clearly different from the one stimulated by TNF and characterized by induction and release of IL-6, CXCL1, CXCL2, and CCL7. This was most pronounced upon exposure to supernatants of 20 Gy-irradiated tumor cells which at the time point of supernatant collection had undergone a late-onset type of primary necrosis.[27] Similar patterns of endothelial cell and/or pericyte activation have been reported in the field of sterile inflammation with models of laser injury and hot needle injury.[42–44] Obviously, the forms of necrotic cell death which are induced by single high dose irradiation, laser injury and hot needle injury as well as the repertoire of released DAMPs share similarities, irrespective if the dying cells are malignant or not. This is further underlined by the dynamics of myeloid cell recruitment: Initially, neutrophils are recruited followed by monocytic cells in a second wave.[45] This seems to be different from intra-tumoral leukocyte recruitment described in the context of anthracycline-based chemotherapy. Here, the crucial mediators have been identified as dying tumor cell-derived ATP, CCL2, and −7, and the authors have not described an initial neutrophil phase.[8,35] Although nucleotides, including ATP, are released from irradiated tumor cells and stimulate chemokinetic monocyte migration *in vitro*, data from this and our previous study suggest that they fail to induce directional monocyte migration and do not contribute to endothelial cell activation.[27] Nevertheless, they may act as local amplifiers of recruitment signals. [46,47]

Neutrophil recruitment by dying tumor cells has been described recently in a mouse model where culture supernatants of tunicamycin- or mitoxanthrone-treated tumor cells were injected into the ear pinnae and in different mouse flank tumors irradiated with high single doses of 15 Gy,[48,49] thus confirming our air pouch findings. The authors of both studies also observed an essential contribution of CXCL1 together with CCL2, CXCL10, and G-CSF. The role of neutrophils recruited by dying tumor cells during radio- and/or chemotherapy still remains to be defined. Yet,

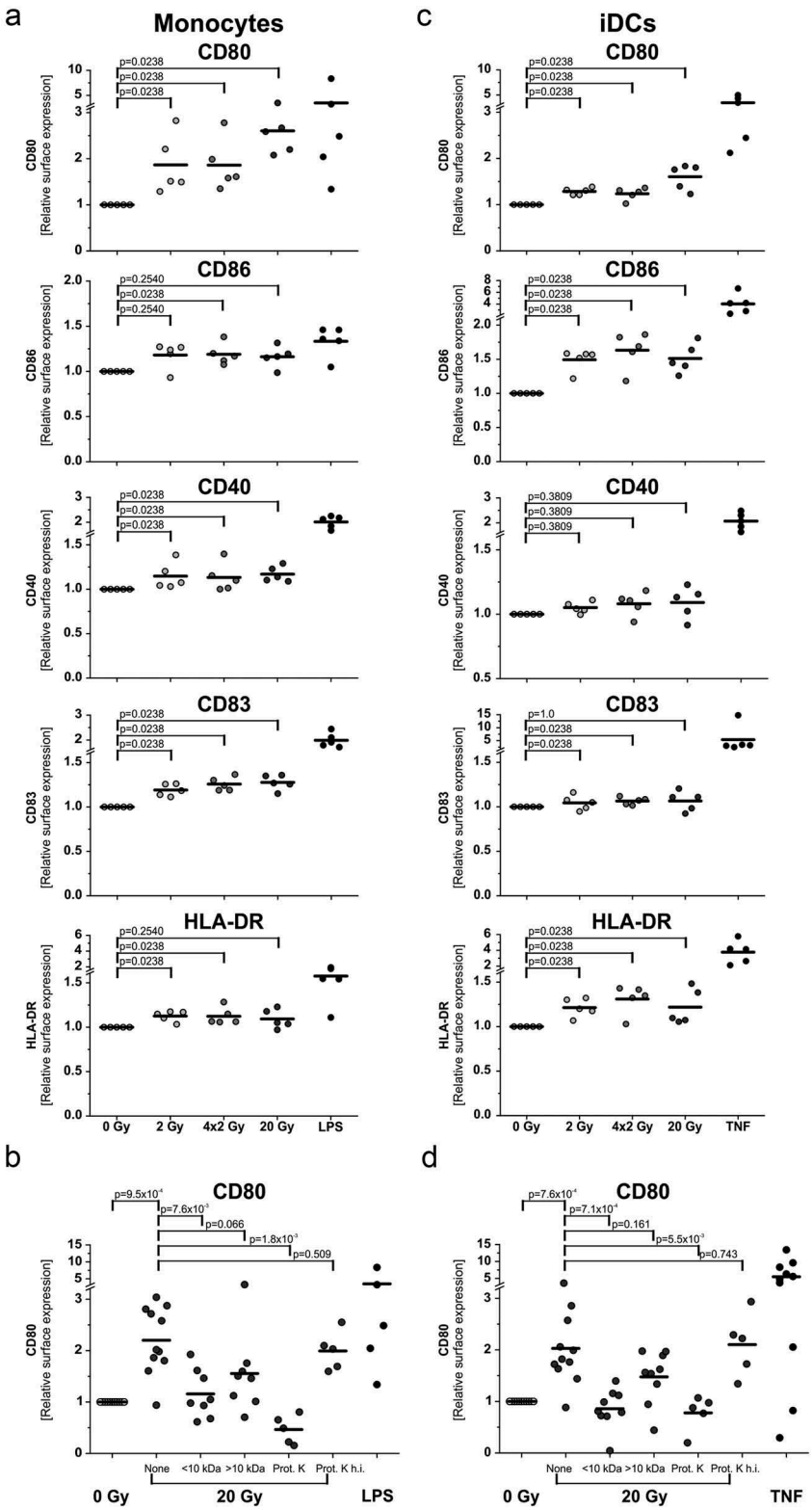

Figure 5. Differentiation and maturation of antigen presenting cells is stimulated by protein DAMPs released from irradiated tumor cells. (a) Differentiation of monocyte-derived DCs. Primary human monocytes were stimulated for 4 h with supernatants of irradiated HCC1937 cells followed by differentiation into DCs with 40 ng/ml IL-4 and 20 ng/ml GM-CSF for 5 days. Surface marker expression was measured by flow cytometry. LPS (200 ng/ml) served as positive control. x-fold increase in surface marker expression was calculated from isotype-subtracted median fluorescence intensities normalized on the corresponding 0 Gy samples. Results from 5 independent experiments are shown, and group comparison was performed by two-sided exact Wilcoxon rank test with Bonferroni-Holm correction. (b) Biochemical characterization of the responsible molecular entities. Supernatants of 20 Gy-irradiated HCC1937 cells were subjected to membrane centrifugation (molecular weight cut-off 10 kDa) and proteinase K digestion prior to incubation with monocytes. CD80 surface expression was determined as in (a). Data from 5–10 independent experiments are shown, and group comparison was performed by two-sided exact Wilcoxon rank test with Bonferroni-Holm correction. (c) Maturation of immature DCs. Immature DCs were differentiated from primary human monocytes with IL-4 (40 ng/ml) and GM-CSF (20 ng/ml) for 5 days. DCs were then stimulated with supernatants of irradiated HCC1937 cells for 2 days and examined by flow cytometry. TNF (100 ng/ml) served as positive control. Data from 5 independent experiments are presented, and *p*-values were calculated by two-sided exact Wilcoxon rank test with Bonferroni-Holm correction. (d) Biochemical characterization. Prior to incubation with DCs, supernatants of 20 Gy-irradiated HCC1937 cells were applied to membrane centrifugation or proteinase K digestion, respectively, as in (b). Data from 5–10 independent experiments are shown, and group comparison was performed by two-sided exact Wilcoxon rank test with Bonferroni-Holm correction.

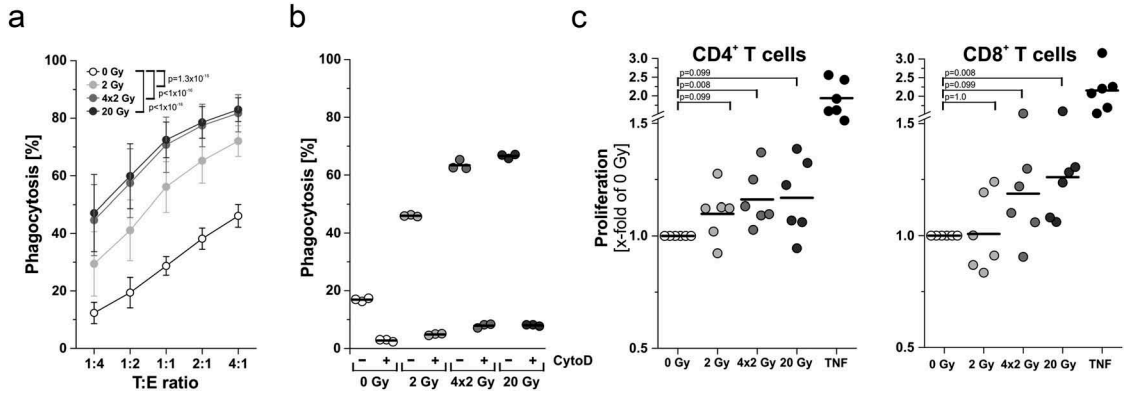

Figure 6. Effector functions of antigen presenting cells are enhanced upon contact with irradiated tumor cells. (a) Phagocytosis and antigen uptake. Immature DCs were differentiated from primary human monocytes (PKH67-labeled) with 40 ng/mL IL-4 and 20 ng/mL GM-CSF for 5 days. Afterwards, DCs were co-incubated with irradiated HCC1937 cells (4 days after irradiation, PKH26-labeled) at the indicated target:effector ratios. Phagocytosis was allowed for 2 h and analyzed by flow cytometry. The percentage of double-positive DCs with ingested HCC1937 cell material is shown as means ± SD of 5 independent experiments. Group comparison was calculated by two-way ANOVA with Bonferroni-Holm correction. (b) DCs were incubated with 20 µM cytochalasin D 1 h prior to performing the phagocytosis assay at a ratio of 1:4 as in (a). (c) Priming of T cell proliferation. DCs were differentiated from primary human monocytes upon exposure to supernatants of irradiated HCC1937 cells or TNF (100 ng/ml) as in Figure 5A. After 7 days, DCs were co-incubated with CFSE-labeled T cells from an allogeneic donor at a ratio of 1:5 (DC:T cells) for additional 5 days before T cell proliferation was analyzed by flow cytometry. The percentage of proliferating T cells was calculated as the percentage of $CD3^+CFSE^{low}CD4^+$ or $CD3^+CFSE^{low}CD8^+$ on the basis of all $CD3^+CD4^+$ or $CD3^+CD8^+$ cells, respectively. Results were normalized on the corresponding 0 Gy samples and are displayed as data from 6 independent experiments. Group comparison was carried out by two-sided exact Wilcoxon rank test with Bonferroni-Holm correction.

evidence is available that neutrophils can engulf dying tumor cells, exert cytotoxic activity against residual, therapy-surviving tumor cells, and thus can contribute to therapy-induced tumor control.[48,49] Additionally, neutrophils are able to create a favorable chemokine milieu for the invasion of monocytic cells and tumor-specific cytotoxic T cells.[45,49]

The role of intra-tumorally recruited monocytic cells in therapeutic settings clearly is subtype-dependent. Anthracycline-based chemotherapy stimulates intra-tumoral infiltration of $Ly6C^{hi}$ monocytic cells which further differentiate into APCs.[8,35] Additionally, $Ly6C^{hi}$ monocytes *per se* appear to be able to efferocytose dying tumor cells and cross-present tumor antigens to $CD8^+$ T cells.[50] However, tumor-promoting monocytic myeloid-derived suppressor cells (MDSCs) also share certain phenotypic similarities with inflammatory $Ly6C^{hi}$ monocytes.[51] A recent study provided evidence that antigen-presenting $Ly6C^{hi}CD103^+$ monocytic cells which accumulate intra-tumorally during immunogenic chemotherapy and exert crucial functions as "first responders" in initiating an anti-tumor response can emerge from tumor-resident MDSC as well as from bone-marrow-derived monocytic precursors.[36] Thus, it will be interesting to dissect the differentiation fate and functionality of the $Ly6C^{hi}$ monocytes that were recruited by supernatants of irradiated tumor cells in our model in greater detail, for instance if they – in the course of differentiation – give rise to the $Ly6C^{lo}$ monocytic population which appeared in the air pouches, or if these cells rather are of tissue-resident origin.[52]

In terms of differentiation and functionality, newly recruited monocytic cells of $CD11c^+CD11b^+Ly6C^{hi}$ phenotype have been shown to upregulate co-stimulatory marker expression and appear to be potent inducers of anti-tumor immunity.[8,36] This is in accordance with our *in vitro* observations with human monocytes whose differentiation into DCs, maturation, and predominantly the upregulation of CD80 and CD86 was enhanced in the presence of supernatants of irradiated tumor cells. Functionally, this was paralleled by improved stimulation of allogeneic $CD8^+$, and to a lesser extent also $CD4^+$ T cells with the strongest effects seen with supernatants of 20 Gy-irradiated tumor cells. These observations are in line with previous reports showing that local and systemic anti-tumor immunity induced by radiotherapy relies on $CD8^+$ T cells.[21,53]

Throughout our study, we observed protein DAMPs with an apparent molecular weight >10 kDa to be responsible for endothelial cell activation, as well as differentiation and maturation of APCs, whereas the migratory activity of monocytic cells in our previous study was mainly controlled by apyrase-sensitive, low-molecular weight nucleotides.[27] Obviously, different classes of DAMPs exert complementary functions, and the details of their contribution require further investigation. Within the class of protein DAMPs, we could detect high levels of HMGB1, HSP70, and S100A8/A9 in the supernatants of irradiated tumor cells. All of them are known to be potent mediators of endothelial cell activation as well as recruitment and differentiation of APCs,[54–56] and they exert their functions via common receptors, including TLR4, the TLR2/4 dimer, RAGE, and members of the scavenger receptor family.[57–59] Accordingly, protein DAMP-stimulated TLR4-signaling has been reported to be essential for anti-tumor immune priming in the context of radiation and chemotherapy.[60,61] Our results on TLR4 activation and its involvement in endothelial cell activation confirm these reports. However, if and to which extent this receptor-ligand axis may be accessible for targeted therapeutic intervention in combined modality approaches of radiotherapy needs to be clarified.

Overall, our study elucidates the early steps of anti-tumor immune priming in the context of cancer radiotherapy and identifies dying cell-derived protein DAMPs, which are most strongly released upon irradiation at high single doses by tumor cells undergoing a delayed type of primary necrosis, as crucial regulators of endothelial cell activation as well as recruitment and differentiation of APCs.

Materials and methods

Primary cells, cell lines, and cell culture supernatants

HCC1937 and HCC1806 cells were obtained from ATCC (Manassas, VA, USA) and cultured in RPMI-1640 medium supplemented with 10% fetal calf serum (FCS), 100 units/ml penicillin, 0.1 mg/ml streptomycin, and 10 mM HEPES (all from Thermo Scientific, Schwerte, Germany) in water-saturated atmosphere at 37°C and 5% CO_2. MDA-MB-436 cells were purchased from CLS (Heidelberg, Germany) and cultured in DMEM/F12 medium supplemented with 10% FCS, 100 units/ml penicillin, and 0.1 mg/ml streptomycin. HEK-Blue™ hTLR2 and HEK-Blue™ hTLR4 reporter cell lines were obtained from InvivoGen (Toulouse, France) and maintained in DMEM medium supplemented with 10% FCS, 50 units/ml penicillin, 0.05 mg/ml streptomycin, 100 µg/ml Normocin™ (InvivoGen), and selection antibiotics. Cell line authentication was performed by short tandem repeat (STR) typing (service provided by the DSMZ, Braunschweig, Germany), and cells were routinely screened to be free from mycoplasma contamination (MycoAlert™ Lonza, Basel, Switzerland). HUVECs were obtained from PromoCell (Heidelberg, Germany) and were grown in full Endothelial Growth Medium (Endothelial Cell Growth Medium plus SupplementMix, both from PromoCell). Human peripheral blood mononuclear cells (PBMCs) were prepared from heparinized blood from healthy donors by density gradient centrifugation (Biocoll density = 1.077 g/ml, Biochrom, Berlin, Germany) as described.[62] Monocytes and T cells were isolated from PBMCs by positive selection with anti-CD14 or anti-CD3 magnetic beads (Miltenyi Biotec, Bergisch Gladbach, Germany), respectively, according to the manufacturer's protocol. Monocytes were differentiated into DCs with 40 ng/ml IL-4 and 20 ng/ml GM-CSF (both from R&D Systems, Heidelberg, Germany) in X-Vivo 15 medium (Lonza) supplemented with 100 units/ml penicillin, 0.1 mg/ml streptomycin, and 10% autologous serum for a minimum of 5 days. IL-4 and GM-CSF were refreshed after 3 days.

Human PMNs were isolated after density gradient centrifugation of heparinized blood from the resulting erythrocyte-granulocyte pellet via hypotonic lysis of erythrocytes (hypotonic buffer: 0.15 M NH_4Cl, 0.01 M $NaHCO_3$, 0.001 M EDTA in H_2O). After washing, freshly isolated PMNs were employed for flow chamber experiments.

The production of cell-free supernatants of x-ray irradiated HCC1937, HCC1806, and MDA-MB-436 cells was described previously.[27] Briefly, 0.5-1x10^6 cells were seeded into 6-well plates, and adherence was allowed overnight. Immediately before x-ray irradiation, cell culture medium was changed to RPMI-1640 or DMEM/F12 medium containing 2.5% FCS, respectively. X-ray irradiation at the indicated doses was performed with an RS225 x-ray cabinet (X-Strahl, Camberley, UK) operated at 200 kV and 10 mA (Thoraeus filter, 1 Gy in 63 s). A single dose of 2 Gy, daily doses of 2 Gy in the fractionated setting, a single ablative dose of 20 Gy, or sham irradiation at 0 Gy were used, respectively. Four days after irradiation, culture supernatants were harvested, cleared by centrifugation (10,000 g, 5 min), and stored at −80°C until further use.

In the biochemical characterization experiments, supernatants of irradiated HCC1937 cells were treated by membrane centrifugation using VivaSpin2 tubes with a molecular weight cut-off of 10 kDa (Sartorius, Goettingen, Germany). Upon centrifugation, both fractions (molecular weight smaller or larger than 10 kDa) were re-adjusted to the initial volume before experiments were performed. Alternatively, the supernatants were digested by 20 µg/ml proteinase K (New England Biolabs, Frankfurt, Germany) for 30 min at 37°C. Proteinase K was subsequently heat-inactivated at 95°C for 50 min. As a control, incubation was carried out with heat-inactivated proteinase K.

HUVEC stimulation was performed with diluted cell-free supernatants of irradiated HCC1937 cells (1:2 in full Endothelial Growth Medium) for 4 h. For cytokine analyses, medium was afterwards replaced, and supernatants were collected after 2 h in order to make sure that HUVECs and not breast cancer cells are the sources of the secreted cytokines. TNF (50 ng/ml, R&D Systems) in full Endothelial Growth Medium served as positive control, and lipopolysaccharide from *R. sphaeroides* (RS-LPS ultrapure, 10 µg/ml, InvivoGen) was used to block activation of TLR4.

Air pouch model

All animal experiments were performed in accordance with the Federation of European Laboratory Animal Science Associations (FELASA) guidelines and were approved by the regional government of Upper Bavaria (Regierungspräsidium Oberbayern). Mice were kept under standard conditions in individually ventilated cages (IVCs) with a 12 h day/night cycle throughout the experiments. Food and water were provided *ad libitum*. Upon air pouch generation, mice were housed individually.

Air pouch generation, stimulation, and harvest

Air pouches were generated by s.c. injection of 5 ml sterile air into the depilated backs of 9–10 weeks old female BALB/c mice. After 3 days, pouch sizes were re-adjusted by injection of 2–3 ml sterile air. Experiments were started 6 days after air pouch generation (Figure 1(a)). 1 ml of air was withdrawn from the pouch and replaced by 1 ml of cell culture supernatant, control medium (RPMI-1640 medium supplemented with 2.5% FCS), or TNF solution (50 ng/ml in RPMI-1640 medium supplemented with 2.5% FCS), respectively. 3 h, 6 h, 12 h, and 24 h after injection, mice were euthanized, and air pouch lavages were collected by washing the pouches with

3 × 2 ml saline (B. Braun, Melsungen, Germany). Afterwards, air pouch skin samples were harvested by surgical excision and fixed in isotonic 3.5% formaldehyde solution for 1 h. Upon washing in PBS, the fixed skin samples were subjected to H&E histochemistry staining or confocal immunofluorescence microscopy, respectively.

H&E histochemistry and confocal immunofluorescence microscopy of air pouch skin samples

For H&E histochemistry, fixed skin samples were embedded in paraffin. 3 µm sections were cut transversally to the muscle fibers, dewaxed in xylene (VWR, Darmstadt, Germany) and rehydrated in a decreasing series of ethanol. Rehydrated sections were stained with hematoxylin staining solution (Merck Millipore, Darmstadt, Germany), and blued in water. Subsequently, skin sections were stained with eosin staining solution (Sigma-Aldrich, Taufkirchen, Germany), followed by dehydration in an increasing ethanol series. Finally, stained sections were embedded in Entellan (Merck Millipore), and microscopy was performed on a Zeiss Lab A1 microscope (Carl Zeiss, Jena, Germany) at 20x magnification.

For confocal immunofluorescence microscopy, fixed air pouch skin samples were first permeabilized in 0.1% Triton X-100 containing 2% BSA (Sigma Aldrich) at 4°C overnight. Skin samples were then stained with anti-F4/80-Alexa Fluor488 (Thermo Scientific), anti-PECAM-1-Alexa Fluor647, and rat anti-Ly6G antibodies (both from BioLegend, Koblenz, Germany) at 4°C for 72 h. Afterwards, samples were washed three times in PBS and incubated with the secondary anti-rat IgG-Alexa Fluor546 antibody (Thermo Scientific) for 3 h at room temperature. The stained samples were washed again, embedded in PermaFluor mounting medium (Thermo Scientific), and subjected to confocal microscopy on a Leica TCS SP5 Confocal microscope (Leica Microsystems, Wetzlar, Germany) at 20x magnification.

Flow cytometry

All flow cytometry experiments were performed on an LSR II cytometer (BD Biosciences, Heidelberg, Germany), and data were analyzed by FACSDiva (BD Biosciences) or Flowjo 7.6.5 software (Tree Star, Ashland, OR, USA), respectively.

Air pouch-infiltrating leukocyte subsets

From air pouch lavages, cells were collected by centrifugation (314 g, 5 min), resuspended in FACS staining buffer (BD Biosciences), and stained with anti-CD45-APC-Cy7, anti-Ly6C-PE-Cy7, anti-Ly6G-BUV395 (all from BD Biosciences), anti-CD11b-FITC, anti-CD11c-PerCP-Cy5.5, anti-F4/80-eFluor450, anti-H-2-Alexa Fluor700, anti-PDCA1-APC, and anti-Siglec-H-PE (all from Thermo Scientific) antibodies or the corresponding isotype controls for 30 min on ice in the dark. Cells were washed twice in FACS staining buffer before FACS analysis was performed. The FACS gating strategy for leukocyte subset identification is depicted in Supplemental Figure 2. Total cell numbers for each leukocyte subset were calculated on the basis of all $CD45^+$ cells counted in the air pouch lavage.

DC surface markers

Monocyte-derived DCs were stained with anti-CD40-PE-Cy5, anti-CD80-PE, anti-CD83-PE-Cy7, anti-CD86-Alexa Fluor700, anti-HLA-DR-PerCP-Cy5.5 antibodies or the matching isotype controls in FACS staining buffer (all from BD Biosciences) for 30 min on ice. After two washing steps with FACS staining buffer, cells were subjected to flow cytometry. Relative surface marker expression was calculated from the median fluorescence intensities subtracted by the corresponding isotype controls and normalized on the 0 Gy controls.

Phagocytosis assays

Phagocytosis assays were performed as reported previously.[63] In brief, isolated primary human monocytes were stained with the green membrane labeling dye PKH67 (Sigma-Aldrich) and differentiated into DCs as described above. HCC1937 cells were stained with the orange membrane labeling dye PKH26 (Sigma-Aldrich) and seeded into 24-well plates (0.3-$1x10^5$ cells/well) prior to irradiation at the indicated doses. Four days after irradiation, DCs were co-incubated with HCC1937 cells in increasing target:effector ratios at 37°C for 2 h. Subsequently, cells were collected by trypsinization and subjected to flow cytometry. The percentage of phagocytosis was determined as the percentage of PKH67/26 double-positive DCs on the basis of all DCs deployed. In order to confirm true engulfment, DCs were incubated with 20 µM of the actin polymerization inhibitor cytochalasin D (Sigma-Aldrich) for 1 h prior to the phagocytosis assay.

Allogeneic mixed leukocyte reaction

Primary human monocytes were stimulated with supernatants of irradiated HCC1937 cells or TNF (100 ng/ml) and differentiated into DCs as described. After 7 days, DCs were seeded into 96-well f-bottom plates ($2x10^4$ cells per well) in 100 µl serum-free X-Vivo 15. On the same day, T cells from an allogeneic blood donor were isolated and labeled with 0.5 µM carboxyfluorescein succinimidyl ester (CFSE, Thermo Scientific) with 1×10^6 T cells/ml in 0.1% BSA in PBS for 10 min at 37°C. Labeled T cells were washed three times in serum-free X-Vivo 15 and added to the DCs in X-Vivo 15 supplemented with 20% autologous serum (ratio DCs:T cells of 1:5) yielding a final volume of 200 µl with 10% autologous serum. Co-incubation was allowed for 5 days. Afterwards, cells were collected, and T cells were stained with anti-CD3-PE-Cy7, anti-CD4-PE, and anti-CD8-APC antibodies or the corresponding isotype controls (all from BD Biosciences) in 50 µl FACS staining buffer for 30 min on ice. Stained T cells were washed twice before flow cytometric analyses. Proliferation of T cells was assessed as the percentage of $CD3^+CD4^+CFSE^{low}$ or $CD3^+CD8^+CFSE^{low}$ T cells on the basis of all $CD3^+CD4^+$ or $CD3^+CD8^+$ T cells, respectively, and normalized on the 0 Gy samples.

Immunofluorescence microscopy

For immunofluorescence analyses, a Carl Zeiss AxioObserver Z1 inverted microscope with an AxioCam Mr3 camera, a

Zeiss Plan-Neofluar 63X/1.3 glycerol objective, an incubator unit XLmulti S1 connected to the heating unit XL S with TempModule S1 and CO2 Module S1, and the AxioVision 4.8 software package (all from Carl Zeiss) was used.

Morphology of breast cancer cells upon irradiation with different regimens

HCC1937 cells were seeded onto sterile cover slips into 24-well plates ($4x10^4$ cells per well) and incubated for adherence overnight. On the next day, HCC1937 cells were irradiated at the indicated doses and fixed on day 1 and 4 after irradiation for 10 min with an isotonic solution of 3.7% formaldehyde (Merck Millipore, Darmstadt, Germany) and 0.1% Triton X-100 (Sigma-Aldrich). After washing in PBS, cells were permeabilized for 5 min in isotonic 0.5% Triton X-100 and subsequently blocked for 1 h with 3% BSA (Sigma-Aldrich) and 0.1% Triton X-100 in PBS. Cells were labeled with Phalloidin-Alexa Fluor568 (Thermo Scientific) and anti-β-tubulin-FITC antibody (Sigma-Aldrich) for 1 h in the dark. Subsequently, labeled cells were washed in 0.1% Triton X-100 in PBS and stained with Hoechst-33342 (2 µg/ml; Sigma-Aldrich) for 5 min. After 4 additional washing steps, slides were mounted with Fluoromount (Sigma-Aldrich) and subjected to microscopy. 25 z-stacks with 250 nm distance were recorded and deconvolved using the AxioVision 4.8 software (applied mode: Iterative).

Adhesion molecule surface expression on endothelial cells

HUVECs were stimulated 48 h after seeding onto sterile coverslips with 400 µl of diluted supernatants of irradiated HCC1937, HCC1806, MDA-MB-436 cells, or TNF, respectively. Upon stimulation, HUVECs were washed with FACS staining buffer before surface staining with anti-intercellular adhesion molecule 1 (ICAM)-1-PE, anti-vascular cell adhesion molecule 1 (VCAM-1)-PE, or anti-E-selectin-PE antibodies (all from BD Biosciences) in FACS staining buffer was allowed for 30 min in the dark. Hoechst-33342 (2 µg/ml) was added for DNA staining. After two washing steps, slides were mounted with Fluoromount and subjected to microscopy.

Live cell imaging

For live cell imaging of phagocytosis, PKH26-labeled HCC1937 cells ($0.3\text{-}1x10^5$ cells/well) were seeded into 8-well µ-slides (ibidi, Martinsried, Germany). Adherence was allowed overnight, and cells were irradiated as described. Phagocytosis by PKH67-labeled DCs was examined 4 d after irradiation with a phagocyte:prey cell ratio of 1:1. Phagocytosis was recorded at 37°C and 5% CO_2 for 3.5 h at 20x magnification. Pictures were taken every 2 min.

Quantification of ICAM-1 and E-selectin surface expression on endothelial cells

HUVECs were seeded into 96-well plates (9,000 cells/well) in full Endothelial Growth Medium and incubated for 48 h. Stimulation was performed with 190 µl of diluted supernatants of irradiated HCC1937 cells for 4 h. Full Endothelial Growth Medium and TNF (50 ng/ml) served as controls. Upon stimulation, cells were washed in FACS staining buffer followed by incubation with anti-ICAM-PE, anti-E-selectin-PE antibodies, or the matching isotype controls for 30 min on ice in the dark. Subsequently, cells were washed twice, and PE-fluorescence was measured on a Synergy Mx plate reader (Ex. 480 nm, Em. 578 nm, BioTek, Berlin, Germany). Relative surface expression of ICAM-1 and E-selectin was calculated from the measured fluorescence intensities subtracted by the corresponding isotype controls and normalized on the 0 Gy samples.

Flow chamber assays

Flow chamber assays were performed as previously described.[64] Briefly, HUVECs were grown in ibidi flow chambers (µ-Slide $VI^{0.4}$)(µ-Slide VI^4) for 48 h. Stimulation was performed with 150 µl of diluted supernatants of irradiated HCC1937 cells or TNF for 4 h. Then, flow chambers were washed twice and perfused with primary human PMNs at a concentration of $2.5x10^3$ cells/ml with a flow rate of 0.11 ml/min (shear force = 0.2 dyn/cm^2). Adherent cells were defined as cells which did not move for more than 1 cell diameter in one minute. This also included crawling cells, which were identified as cells moving less than 1 cell diameter/min.

Cytokine multiplex-ELISA

Concentrations of cytokines in supernatants of stimulated HUVECs were measured with the Bio-Plex Pro Human Chemokine Assay on a Bio-Plex 200 system according to the manufacturer's protocol (Bio-Rad Laboratories, Munich, Germany). Stimulation of HUVECs was performed in 6-well plates ($2x10^5$ cells per well) with 2 ml of diluted supernatants of irradiated HCC1937 cells for 4 h. Afterwards, medium was changed to full Endothelial Growth Medium, and cell culture supernatants were collected after 2h.

HSP70, HMGB1, and S100A8/A9 ELISA

Levels of HSP70 and HMGB1 in supernatants of irradiated HCC1937, HCC1806, and MDA-MB-436 cells were measured with the HSP70-DuoSet-ELISA kit (R&D Systems) and the HMGB1-ELISA kit (IBL International, Hamburg, Germany) according to the manufacturers' protocols. S100A8/9 protein levels were quantified as described.[65]

Quantitative realtime PCR

qRT-PCR was performed as reported previously.[27] From air pouch skin samples, total RNA was extracted with TRIzol Reagent (Thermo Scientific) according to the manufacturer's protocol. From *in vitro* HUVEC experiments total RNA was isolated with the NucleoSpin RNA II-Kit (Macherey and Nagel, Dueren, Germany). Afterwards, 1 µg of total RNA was reversely transcribed with 200 U Revert Aid H Minus M-MuLV reverse transcriptase in the presence of 5 µM random hexamers, 5 µM $Oligo(dT)_{18}$, 1 U/µl Ribolock RNase inhibitor (all from Thermo Scientific), and 500µM dNTPs (Promega, Heidelberg, Germany) in a final volume of 20 µl or 50 µl, respectively. For qRT-PCR, the resulting cDNA (20–80 ng) was mixed with 300 nM forward and

reverse primers (all synthesized by Sigma-Aldrich), and amplification was performed in 1x Maxima SYBR Green qPCR Master Mix (Thermo Scientific) in a final volume of 20 µl with a standard cycling protocol (10 min 95°C, 45x (15 s 95°C, 30 s 60°C)) on an LC480 qPCR cycler (Roche Applied Science, Penzberg, Germany). The primer sequences for mouse and human target genes are listed in Supplemental Tables 1 and 2. Relative quantification was performed using the standard curve method, the results were normalized on a matrix of 3–5 reference genes as indicated, and calibrated on the given controls.

Detection of TLR activation by HEK-Blue™hTLR2 and HEK-Blue™ hTLR4 reporter cell lines

HEK-Blue™ hTLR cells were seeded in HEK-Blue™ Detection medium into 96-well plates (50,000 cells/well) which were pre-filled with 20 µl culture supernatants of irradiated breast cancer cell lines. LPS (10 ng/ml) or fibroblast-stimulating lipopeptide-1 (FSL-1, Pam2CGDPKHPKSF, 10 ng/ml, InvivoGen) served as positive controls for hTLR4 or hTLR2 activation, respectively. TLR stimulation was allowed for 7 h at 37°C. Subsequently, activity of secreted alkaline phosphatase (SEAP) was measured kinetically in a Synergy MX plate reader (10 h at 37°C, absorption at 630nm, measurement every 2 min at 37°C) and calculated from the slope of the corresponding regression lines. Relative TLR activation was expressed as x-fold values of samples treated with 0 Gy culture supernatants.

Statistical analyses

Data are presented as independent data points from individual experiments unless stated otherwise. For time course experiments, means ± standard deviation (SD) or standard error of the mean (SEM) of the indicated number of animals or independent experiments are shown. Normal distribution was confirmed by Kolmogorov-Smirnov analysis, and group comparisons were performed by two-tailed, unpaired Student's *t*-test or two-way ANOVA, respectively. If normality was rejected, two-sided exact Wilcoxon rank test was employed. Multiple testing correction was performed using the *post hoc* Bonferroni-Holm algorithm. Principal component analysis (PCA) was carried out in OriginPro 9.1 as previously described.[66]

Acknowledgments

This work was supported by the DFG (SFB914 Project B06 to KL, B03 to CAS, and B06 to MS, INST 409/22-1 FUGG, INST 409/20-1 FUGG, and INST 409/126-1 FUGG to CB and KL) and the BMBF (ZiSS 02NUK024C and ZiSStrans 02NUK047C to KL and CB). We thank Manfred Felbermeier for excellent technical assistance during animal experiments. Data presented in this study are part of the doctoral theses of JK, RH and NB.

Funding

This work was supported by the Deutsche Forschungsgemeinschaft (DFG) [INST 409/22-1 FUGG, INST 409/20-1 FUGG, and INST 409/126-1 FUGG];BMBF [ZiSS 02NUK024C and ZiSStrans 02NUK047C];Deutsche Forschungsgemeinschaft (DFG) [SFB914 project B01, B03, B06].

Conflict of Interest

The authors declare that conflicts of interest do not exist.

Abbreviations

APC	antigen-presenting cell
CFSE	Carboxyfluorescein succinimidyl ester
cGAS	cyclic GMP-AMP synthase
DAMPs	damage-associated molecular patterns
DC	dendritic cell
FCS	fetal calf serum
FSL-1	fibroblast-stimulating lipopeptide (Pam2CGDPKHPKSF)
H&E	hematoxylin/eosin
HMGB1	high mobility group box 1
HSP70	heat shock protein 70
HUVEC	human umbilical vein endothelial cell
ICAM-1	intercellular adhesion molecule 1
LPS	Lipopolysaccharide
PBMC	peripheral blood mononuclear cell
PCA	principal component analysis
PECAM-1	platelet endothelial cell adhesion molecule 1
PML	polymorphonuclear leukocytes
PMN	polymorphonuclear neutrophils
qRT-PCR	quantitative real time polymerase chain reaction
RS-LPS	lipopolysaccharide from *R. sphaeroides*
SD	standard deviation
SEM	standard error of the mean
SEAP	secreted alkaline phosphatase
STING	stimulator of interferon genes
TNF	tumor necrosis factor
TLR	toll-like receptor
VCAM-1	vascular cell adhesion protein 1

Authors Contribution

KL, CB, RH, JK, CAR, and MS conceived and designed experiments. JK, RH, NB, MO, US, AE, JS, GZ, SB, and TV performed experiments and analyzed the data. SU performed sample size calculations and provided statistical consulting. RH, JK and KL wrote the manuscript, and all authors discussed the results and commented on the manuscript.

ORCID

Roman Hennel http://orcid.org/0000-0002-0362-6952
Markus Sperandio http://orcid.org/0000-0002-7689-3613
Steffen Unkel http://orcid.org/0000-0002-2083-0090

References

1. Orth M, Lauber K, Niyazi M, Friedl AA, Li M, Maihofer C, Schuttrumpf L, Ernst A, Niemoller OM, Belka C. Current concepts in clinical radiation oncology. Radiat Environ Biophys. 2014;53:1–29.doi:10.1007/s00411-013-0497-2.
2. Garg AD, Romano E, Rufo N, Agostinis P. Immunogenic versus tolerogenic phagocytosis during anticancer therapy: mechanisms and clinical translation. Cell Death Differ. 2016;23:938–951. doi:10.1038/cdd.2016.5.
3. Lauber K, Ernst A, Orth M, Herrmann M, Belka C. Dying cell clearance and its impact on the outcome of tumor radiotherapy. Front Oncol. 2012;2:116. doi:10.3389/fonc.2012.00116.

4. Demaria S, Formenti SC. Radiation as an immunological adjuvant: current evidence on dose and fractionation. Front Oncol. 2012;2:153. doi:10.3389/fonc.2012.00153.
5. Chen DS, Mellman I. Oncology meets immunology: the cancer-immunity cycle. Immunity. 2013;39:1–10. doi:10.1016/j.immuni.2013.07.012.
6. Brix N, Tiefenthaller A, Anders H, Belka C, Lauber K. Abscopal, immunological effects of radiotherapy: narrowing the gap between clinical and preclinical experiences. Immunol Rev. 2017;280:249–279. doi:10.1111/imr.12573.
7. Galluzzi L, Buqué A, Kepp O, Zitvogel L, Kroemer G. Immunogenic cell death in cancer and infectious disease. Nat Rev Immunol. 2017;17:97–111. doi:10.1038/nri.2016.107.
8. Ma Y, Adjemian S, Mattarollo SR, Yamazaki T, Aymeric L, Yang H, Portela Catani JP, Hannani D, Duret H, Steegh K, et al. Anticancer chemotherapy-induced intratumoral recruitment and differentiation of antigen-presenting cells. Immunity. 2013;38:729–741. doi:10.1016/j.immuni.2013.03.003.
9. Di Blasio S, Wortel IMN, van Bladel DAG, de Vries LE, Duiveman-de Boer T, Worah K, de Haas N, Buschow SI, de Vries IJ, Figdor CG, et al. Human CD1c(+) DCs are critical cellular mediators of immune responses induced by immunogenic cell death. Oncoimmunology. 2016;5:e1192739. doi:10.1080/2162402X.2016.1192739.
10. Eriksson D, Stigbrand T. Radiation-induced cell death mechanisms. Tumour Biol. 2010;31:363–372. doi:10.1007/s13277-010-0042-8.
11. Galluzzi L, Vitale I, Aaronson SA, Abrams JM, Adam D, Agostinis P, Alnemri ES, Altucci L, Amelio I, Andrews DW, et al. Molecular mechanisms of cell death: recommendations of the nomenclature committee on cell death 2018. Cell Death Differ. 2018;25:486–541. doi:10.1038/s41418-017-0012-4.
12. Vandenabeele P, Vandecasteele K, Bachert C, Krysko O, Krysko DV. Immunogenic apoptotic cell death and anticancer immunity. Adv Exp Med Biol. 2016;930:133–149. doi:10.1007/978-3-319-39406-0_6.
13. Kuilman T, Michaloglou C, Mooi WJ, Peeper DS. The essence of senescence. Genes Dev. 2010;24:2463–2479. doi:10.1101/gad.1971610.
14. Krysko O, Aaes TL, Kagan VE, D'Herde K, Bachert C, Leybaert L, Vandenabeele P, Krysko DV. Necroptotic cell death in anti-cancer therapy. Immunol Rev. 2017;280:207–219. doi:10.1111/imr.12583.
15. Mole RH. Whole body irradiation; radiobiology or medicine? Br J Radiol. 1953;26:234–241. doi:10.1259/0007-1285-26-305-234.
16. Demaria S, Ng B, Devitt ML, Babb JS, Kawashima N, Liebes L, Formenti SC. Ionizing radiation inhibition of distant untreated tumors (abscopal effect) is immune mediated. Int J Radiat Oncol Biol Phys. 2004;58:862–870. doi:10.1016/j.ijrobp.2003.09.012.
17. Golden EB, Frances D, Pellicciotta I, Demaria S, Helen Barcellos-Hoff M, Formenti SC. Radiation fosters dose-dependent and chemotherapy-induced immunogenic cell death. Oncoimmunology. 2014;3:e28518. doi:10.4161/onci.28518.
18. Deng L, Liang H, Xu M, Yang X, Burnette B, Arina A, Li X-D, Mauceri H, Beckett M, Darga T, et al. STING-dependent cytosolic DNA sensing promotes radiation-induced type I interferon-dependent antitumor immunity in immunogenic tumors. Immunity. 2014;41:843–852. doi:10.1016/j.immuni.2014.10.019.
19. Sistigu A, Yamazaki T, Vacchelli E, Chaba K, Enot DP, Adam J, Vitale I, Goubar A, Baracco EE, Remédios C, et al. Cancer cell-autonomous contribution of type I interferon signaling to the efficacy of chemotherapy. Nat Med. 2014;20:1301–1309. doi:10.1038/nm.3708.
20. Burnette BC, Liang H, Lee Y, Chlewicki L, Khodarev NN, Weichselbaum RR, Fu Y-X, Auh SL. The efficacy of radiotherapy relies upon induction of type i interferon-dependent innate and adaptive immunity. Cancer Res. 2011;71:2488–2496. doi:10.1158/0008-5472.CAN-10-2820.
21. Lee Y, Auh SL, Wang Y, Burnette B, Wang Y, Meng Y, Beckett M, Sharma R, Chin R, Tu T, et al. Therapeutic effects of ablative radiation on local tumor require CD8+ T cells: changing strategies for cancer treatment. Blood. 2009;114:589–595. doi:10.1182/blood-2009-02-206870.
22. Lugade AA, Moran JP, Gerber SA, Rose RC, Frelinger JG, Lord EM. Local radiation therapy of B16 melanoma tumors increases the generation of tumor antigen-specific effector cells that traffic to the tumor. J Immunol. 2005;174:7516–7523.
23. Lugade AA, Sorensen EW, Gerber SA, Moran JP, Frelinger JG, Lord EM. Radiation-induced IFN-gamma production within the tumor microenvironment influences antitumor immunity. J Immunol. 2008;180:3132–3139.
24. Vanpouille-Box C, Alard A, Aryankalayil MJ, Sarfraz Y, Diamond JM, Schneider RJ, Inghirami G, Coleman CN, Formenti SC, Demaria S. DNA exonuclease Trex1 regulates radiotherapy-induced tumour immunogenicity. Nat Commun. 2017;8:15618. doi:10.1038/ncomms15618.
25. Foulkes WD, Smith IE, Reis-Filho JS. Triple-negative breast cancer. N Engl J Med. 2010;363:1938–1948. doi:10.1056/NEJMra1001389.
26. Stoll G, Ma Y, Yang H, Kepp O, Zitvogel L, Kroemer G. Pro-necrotic molecules impact local immunosurveillance in human breast cancer. Oncoimmunology. 2017;6:e1299302. doi:10.1080/2162402X.2017.1299302.
27. Hennel R, Brix N, Seidl K, Ernst A, Scheithauer H, Belka C, Lauber K. Release of monocyte migration signals by breast cancer cell lines after ablative and fractionated gamma-irradiation. Radiat Oncol. 2014;9:85. doi:10.1186/1748-717X-9-85.
28. Ley K, Laudanna C, Cybulsky MI, Nourshargh S. Getting to the site of inflammation: the leukocyte adhesion cascade updated. Nat Rev Immunol. 2007;7:678–689. doi:10.1038/nri2156.
29. Eue I, Pietz B, Storck J, Klempt M, Sorg C. Transendothelial migration of 27E10+ human monocytes. Int Immunol. 2000;12:1593–1604.
30. Bianchi ME, Manfredi AA. High-mobility group box 1 (HMGB1) protein at the crossroads between innate and adaptive immunity. Immunol Rev. 2007;220:35–46. doi:10.1111/j.1600-065X.2007.00574.x.
31. Tsan MF, Gao B. Heat shock proteins and immune system. J Leukoc Biol. 2009;85:905–910. doi:10.1189/jlb.0109005.
32. Peter C, Wesselborg S, Herrmann M, Lauber K. Dangerous attraction: phagocyte recruitment and danger signals of apoptotic and necrotic cells. Apoptosis. 2010;15:1007–1028. doi:10.1007/s10495-010-0472-1.
33. Menezes S, Melandri D, Anselmi G, Perchet T, Loschko J, Dubrot J, Patel R, Gautier EL, Hugues S, Longhi MP, et al. The heterogeneity of Ly6C(hi) monocytes controls their differentiation into iNOS(+) macrophages or monocyte-derived dendritic cells. Immunity. 2016;45:1205–1218. doi:10.1016/j.immuni.2016.12.001.
34. Chen L, Flies DB. Molecular mechanisms of T cell co-stimulation and co-inhibition. Nat Rev Immunol. 2013;13:227–242. doi:10.1038/nri3405.
35. Ma Y, Mattarollo SR, Adjemian S, Yang H, Aymeric L, Hannani D, Portela Catani JP, Duret H, Teng MWL, Kepp O, et al. CCL2/CCR2-dependent recruitment of functional antigen-presenting cells into tumors upon chemotherapy. Cancer Res. 2014;74:436–445. doi:10.1158/0008-5472.CAN-13-1265.
36. Sharma MD, Rodriguez PC, Koehn BH, Baban B, Cui Y, Guo G, Shimoda M, Pacholczyk R, Shi H, Lee EJ, et al. Activation of p53 in immature myeloid precursor cells controls differentiation into Ly6c(+)CD103(+) monocytic antigen-presenting cells in tumors. Immunity. 2018;48:91–106 e6. doi:10.1016/j.immuni.2017.12.014.
37. Darby S, Darby S, McGale P, Correa C, Taylor C, Arriagada R, Clarke M, Cutter D, Davies C, Ewertz M, et al. Effect of radiotherapy after breast-conserving surgery on 10-year recurrence and 15-year breast cancer death: meta-analysis of individual patient data for 10,801 women in 17 randomised trials. Lancet. 2011;378:1707–1716. doi:10.1016/S0140-6736(11)61629-2.
38. Barker HE, Paget JTE, Khan AA, Harrington KJ. The tumour microenvironment after radiotherapy: mechanisms of resistance and recurrence. Nat Rev Cancer. 2015;15:409–425. doi:10.1038/nrc3958.
39. Dewan MZ, Galloway AE, Kawashima N, Dewyngaert JK, Babb JS, Formenti SC, Demaria S. Fractionated but not single-dose radiotherapy induces an immune-mediated abscopal effect when

combined with anti-CTLA-4 antibody. Clin Cancer Res. 2009;15:5379–5388. doi:10.1158/1078-0432.CCR-09-0265.
40. Filatenkov A, Baker J, Mueller AMS, Kenkel J, Ahn G-O, Dutt S, Zhang N, Kohrt H, Jensen K, Dejbakhsh-Jones S, et al. Ablative tumor radiation can change the tumor immune cell microenvironment to induce durable complete remissions. Clin Cancer Res. 2015;21:3727–3739. doi:10.1158/1078-0432.CCR-14-2824.
41. Schaue D, Ratikan JA, Iwamoto KS, McBride WH. Maximizing tumor immunity with fractionated radiation. Int J Radiat Oncol Biol Phys. 2012;83:1306–1310. doi:10.1016/j.ijrobp.2011.09.049.
42. Pittman K, Kubes P. Damage-associated molecular patterns control neutrophil recruitment. J Innate Immun. 2013;5:315–323. doi:10.1159/000347132.
43. McDonald B, Pittman K, Menezes GB, Hirota SA, Slaba I, Waterhouse CCM, Beck PL, Muruve DA, Kubes P. Intravascular danger signals guide neutrophils to sites of sterile inflammation. Science. 2010;330:362–366. doi:10.1126/science.1195491.
44. Stark K, Eckart A, Haidari S, Tirniceriu A, Lorenz M, von BM-L, Gärtner F, Khandoga AG, Legate KR, Pless R, et al. Capillary and arteriolar pericytes attract innate leukocytes exiting through venules and 'instruct' them with pattern-recognition and motility programs. Nat Immunol. 2013;14:41–51. doi:10.1038/ni.2477.
45. Soehnlein O, Lindbom L, Weber C. Mechanisms underlying neutrophil-mediated monocyte recruitment. Blood. 2009;114:4613–4623. doi:10.1182/blood-2009-06-221630.
46. Isfort K, Ebert F, Bornhorst J, Sargin S, Kardakaris R, Pasparakis M, Bähler M, Schwerdtle T, Schwab A, Hanley PJ. Real-time imaging reveals that P2Y2 and P2Y12 receptor agonists are not chemoattractants and macrophage chemotaxis to complement C5a is phosphatidylinositol 3-kinase (PI3K)- and p38 mitogen-activated protein kinase (MAPK)-independent. J Biol Chem. 2011;286:44776–44787. doi:10.1074/jbc.M111.289793.
47. Kronlage M, Song J, Sorokin L, Isfort K, Schwerdtle T, Leipziger J, Robaye B, Conley PB, Kim H-C, Sargin S, et al. Autocrine purinergic receptor signaling is essential for macrophage chemotaxis. Sci Signal. 2010;3:ra55. doi:10.1126/scisignal.2000588.
48. Garg AD, Vandenberk L, Fang S, Fasche T, Van Eygen S, Maes J, Van Woensel M, Koks C, Vanthillo N, Graf N, et al. Pathogen response-like recruitment and activation of neutrophils by sterile immunogenic dying cells drives neutrophil-mediated residual cell killing. Cell Death Differ. 2017;24:832–843. doi:10.1038/cdd.2017.15.
49. Takeshima T, Pop LM, Laine A, Iyengar P, Vitetta ES, Hannan R. Key role for neutrophils in radiation-induced antitumor immune responses: potentiation with G-CSF. Proc Natl Acad Sci U S A. 2016;113:11300–11305. doi:10.1073/pnas.1613187113.
50. Larson SR, Atif SM, Gibbings SL, Thomas SM, Prabagar MG, Danhorn T, Leach SM, Henson PM, Jakubzick CV. Ly6C(+) monocyte efferocytosis and cross-presentation of cell-associated antigens. Cell Death Differ. 2016;23:997–1003. doi:10.1038/cdd.2016.24.
51. Youn J-I, Nagaraj S, Collazo M, Gabrilovich DI. Subsets of myeloid-derived suppressor cells in tumor-bearing mice. J Immunol. 2008;181:5791–5802.
52. Merad M, Sathe P, Helft J, Miller J, Mortha A. The dendritic cell lineage: ontogeny and function of dendritic cells and their subsets in the steady state and the inflamed setting. Annu Rev Immunol. 2013;31:563–604. doi:10.1146/annurev-immunol-020711-074950.
53. Gupta A, Probst HC, Vuong V, Landshammer A, Muth S, Yagita H, Schwendener R, Pruschy M, Knuth A, van Den Broek M. Radiotherapy promotes tumor-specific effector CD8+ T cells via dendritic cell activation. J Immunol. 2012;189:558–566. doi:10.4049/jimmunol.1200563.
54. Bianchi ME, Crippa MP, Manfredi AA, Mezzapelle R, Rovere Querini P, Venereau E. High-mobility group box 1 protein orchestrates responses to tissue damage via inflammation, innate and adaptive immunity, and tissue repair. Immunol Rev. 2017;280:74–82. doi:10.1111/imr.12601.
55. Joly A-L, Wettstein G, Mignot G, Ghiringhelli F, Garrido C. Dual role of heat shock proteins as regulators of apoptosis and innate immunity. J Innate Immun. 2010;2:238–247. doi:10.1159/000296508.
56. Viemann D, Strey A, Janning A, Jurk K, Klimmek K, Vogl T, Hirono K, Ichida F, Foell D, Kehrel B, et al. Myeloid-related proteins 8 and 14 induce a specific inflammatory response in human microvascular endothelial cells. Blood. 2005;105:2955–2962. doi:10.1182/blood-2004-07-2520.
57. Fiuza C, Bustin M, Talwar S, Tropea M, Gerstenberger E, Shelhamer JH, Suffredini AF. Inflammation-promoting activity of HMGB1 on human microvascular endothelial cells. Blood. 2003;101:2652–2660. doi:10.1182/blood-2002-05-1300.
58. Vogel S, Börger V, Peters C, Förster M, Liebfried P, Metzger K, Meisel R, Däubener W, Trapp T, Fischer JC, et al. Necrotic cell-derived high mobility group box 1 attracts antigen-presenting cells but inhibits hepatocyte growth factor-mediated tropism of mesenchymal stem cells for apoptotic cell death. Cell Death Differ. 2015;22:1219–1230. doi:10.1038/cdd.2014.225.
59. Chakraborty D, Zenker S, Rossaint J, Hölscher A, Pohlen M, Zarbock A, Roth J, Vogl T. Alarmin S100A8 activates alveolar epithelial cells in the context of acute lung injury in a TLR4-dependent manner. Front Immunol. 2017;8:1493. doi:10.3389/fimmu.2017.01493.
60. Apetoh L, Ghiringhelli F, Tesniere A, Obeid M, Ortiz C, Criollo A, Mignot G, Maiuri MC, Ullrich E, Saulnier P, et al. Toll-like receptor 4-dependent contribution of the immune system to anticancer chemotherapy and radiotherapy. Nat Med. 2007;13:1050–1059. doi:10.1038/nm1622.
61. Chen T, Guo J, Han C, Yang M, Cao X. Heat shock protein 70, released from heat-stressed tumor cells, initiates antitumor immunity by inducing tumor cell chemokine production and activating dendritic cells via TLR4 pathway. J Immunol. 2009;182:1449–1459.
62. Lauber K, Keppeler H, Munoz LE, Koppe U, Schröder K, Yamaguchi H, Krönke G, Uderhardt S, Wesselborg S, Belka C, et al. Milk fat globule-EGF factor 8 mediates the enhancement of apoptotic cell clearance by glucocorticoids. Cell Death Differ. 2013;20:1230–1240. doi:10.1038/cdd.2013.82.
63. Rosenwald M, Koppe U, Keppeler H, Sauer G, Hennel R, Ernst A, Blume KE, Peter C, Herrmann M, Belka C, et al. Serum-derived plasminogen is activated by apoptotic cells and promotes their phagocytic clearance. J Immunol. 2012;189:5722–5728. doi:10.4049/jimmunol.1200922.
64. Nussbaum C, Gloning A, Pruenster M, Frommhold D, Bierschenk S, Genzel-Boroviczény O, von Andrian UH, Quackenbush E, Sperandio M. Neutrophil and endothelial adhesive function during human fetal ontogeny. J Leukoc Biol. 2013;93:175–184. doi:10.1189/jlb.0912468.
65. Frosch M, Strey A, Vogl T, Wulffraat NM, Kuis W, Sunderkötter C, Harms E, Sorg C, Roth J. Myeloid-related proteins 8 and 14 are specifically secreted during interaction of phagocytes and activated endothelium and are useful markers for monitoring disease activity in pauciarticular-onset juvenile rheumatoid arthritis. Arthritis Rheum. 2000;43:628–637. doi:10.1002/1529-0131(200003)43:3<628::AID-ANR20>3.0.CO;2-X.
66. Ernst A, Anders H, Kapfhammer H, Orth M, Hennel R, Seidl K, Winssinger N, Belka C, Unkel S, Lauber K. HSP90 inhibition as a means of radiosensitizing resistant, aggressive soft tissue sarcomas. Cancer Lett. 2015;365:211–222. doi:10.1016/j.canlet.2015.05.024.